Electronic Supplementary Information (ESI) for:

Adducts of Triangular Silver(I) 3,5-Bis(trifluoromethyl)pyrazolate with Thiophene-Derivatives: A Weak Interaction Model of Desulfurization

Rongrong Liu,[a] Wenhua Zhang,[a] Donghui Wei,[a] Jing-Huo Chen*,[a] Seik Weng Ng,[b] Guang Yang*[a]

* yang@zzu.edu.cn; jhchen@zzu.edu.cn

[a] College of Chemistry, Zhengzhou University, Henan, Zhengzhou, 450001, P. R. China.

[b] Department of Chemistry University of Malaya, Kuala Lumpur, Malaysia.

Measurements and instruments

All commercial materials were used as received without further purification. NMR spectra were recorded on a Bruker DPX-600 spectrometer. Powder X-ray diffraction (PXRD) data were collected using a PANalytical X-Pert Pro powder diffractometer with Cu Kα radiation. The Fourier transform infrared (FT-IR) spectra were obtained in the range 400-4000 cm^{-1} on a Nicolet NEXUS 470-FTIR spectrophotometer using KBr pellets. Thermogravimetric analyses (TGA) were conducted on a Netzsch STA 449 F5 by heating the sample from 40 to 800 °C under nitrogen at a rate of 20 °C•min^{-1}. The Ag content was analyzed by means of an Agilent inductively coupled plasma (ICP) OES730 spectrometer. DBT and DMDBT contents were determined by Agilent 1100 HPLC system.

Experimental Procedures

Synthesis of Ag_3pz_3·DBT

Ag_3pz_3 (0.012 mmol, 11.2 mg) and DBT (0.024 mmol, 4.4 mg) were dissolved in 2 mL of dichloromethane. The solution was allowed to slow evaporation at 5 °C for 2 days to afford the colorless needle crystals of **Ag_3pz_3·DBT** along with some unreacted DBT crystals. The pure sample of **Ag_3pz_3·DBT** can be obtained by washing the mixture with petroleum ether. Yield: 11.7 mg, 0.0104 mmol, 87%. Mp: 201-203 °C (melts with dec.) ^{1}H NMR (600 MHz, CD_2Cl_2): δ 8.06 (d, J = 7.7 Hz, 2H, Ph), 7.69 (d,J = 7.7 Hz, 2H, Ph), 7.42 (t, J = 7.2 Hz, 2H, Ph), 7.38 (t, J = 7.5 Hz, 2H, Ph), 7.07 (s, 3H, Pz-H) ppm. ^{13}C NMR (151 MHz, CD_2Cl_2): δ 139.44 (s, Thienyl), 135.78 (s, Thienyl), 127.37 (s, Ph), 125.04 (s, Ph), 123.22 (s, Ph), 121.98 (s, Ph), 120.86 (q, $^1J_{CF}$ = 270.29 Hz, CF_3), 103.57(s, Pz-C_4) ppm.

Synthesis of Ag_3pz_3·DMDBT

This adduct was prepared in a similar way as for **Ag_3pz_3·DBT**, using DMDBT (0.024 mmol, 5.1 mg) instead of DBT. Yield: 12.4 mg, 0.0108 mmol, 90%. Mp: 207-210 °C (melts with dec.) ^{1}H NMR (600 MHz, CD_2Cl_2): δ 7.84 (d, J = 7.8 Hz, 2H, Ph), 7.34 (t, J = 7.5 Hz, 2H, Ph), 7.19 (d, J = 7.1 Hz, 2H, Ph), 7.07 (s, 3H, Pz-H), 2.41 (s, 6H, CH_3) ppm. ^{13}C NMR (151 MHz, CD_2Cl_2): δ 139.39 (s, Thienyl), 136.20 (s, Thienyl), 133.15 (s, Ph), 127.64 (s, Ph), 125.54(s, Ph), 119.56 (s, Ph), 120.86 (q, $^1J_{CF}$ = 269.79 Hz, CF_3), 103.60(s, Pz-C_4), 20.41(s, CH_3) ppm.

Synthesis of Ag_3pz_3·BT

This adduct was obtained as pure phase in a similar way as for **Ag_3pz_3·DBT**, using BT (0.06 mmol, 8.1 mg) instead of DBT within a week. Yield: 10.5 mg, 0.0098 mmol, 82%. Mp: 167-169 °C (melts with dec.) ^{1}H NMR (600 MHz, CD_2Cl_2): δ 7.86 (d, J = 7.5 Hz, 1H, Ph), 7.80 (d, J = 7.4 Hz, 1H, Ph), 7.43 (d, J = 5.3 Hz, 1H, Thienyl), 7.34 (m, 3H, J = 6.9 Hz, Ph and Thienyl), 7.09 (s, 3H, Pz-H) ppm. ^{13}C NMR (151 MHz, CD_2Cl_2): δ 144.90 (q, $^2J_{CF}$ = 35.74 Hz, $C$$CF_3$), 140.05 (s, Thienyl), 140.01(s, Thienyl), 126.82 (s, Thienyl), 124.72 (s, Ph), 124.69 (s, Ph), 124.34 (s, Thienyl), 124.04(s, Ph), 122.85 (s, Ph), 120.87 (q, $^1J_{CF}$ = 267.77 Hz, CF_3), 103.65 (s, Pz-C_4) ppm.

Synthesis of Ag_3pz_3·DMT

This adduct was obtained as pure phase in a similar way as for the **Ag_3pz_3·DBT**, using DMT (0.36 mmol, 42 μL) instead of DBT within a week. Yield: 10.7 mg, 0.0102 mmol, 85%. Mp: 178-180 °C (melts with dec.) ^{1}H NMR (600 MHz, CD_2Cl_2): δ 7.09 (s, 3H, Pz-H), 6.51 (s, 2H, Thienyl), 2.39 (s, 6H, CH_3) ppm. ^{13}C NMR (151 MHz, CD_2Cl_2): δ 144.99 (q, $^2J_{CF}$ = 36.8 Hz, $C$$CF_3$), 137.96 (s, DMT-C), 125.24 (s, DMT-CH), 120.90 (q, $^1J_{CF}$ = 269.28 Hz, CF_3), 103.67 (s, Pz-C_4), 15.29 (s, DMT-CH_3) ppm.

Desulfurization Performance

1.3 Equivalent amount of **Ag_3pz_3** was added to 10 mL of model oil (isooctane containing 100 mg/L S of DBT or DMDBT), white precipitate formed immediately, which was kept stirring for 0.5 h (Fig. S23-S24). The precipitate was isolated from the oil by centrifugation, which proved to be the 1:1 adduct, as verified by ^{1}HNMR and PXRD. From the mass of the precipitate, it is estimated that 91.7 % of DBT or 89.9 % DMDBT have been removed from oil at this stage. The remaining **Ag_3zp_3** and DBT/DMDBT in the oil can be further treated by acetonitrile extraction. By this desulfurization scheme, the S-content can be reduced from 100 mg/L S to 0.55 mg/L S and 1.50 mg/L S for DBT and DMDBT, respectively, and ICP measurement shows no detectable Ag^+ atoms left in the oil after treatment.

Recyclable Performance

The recycling of Ag_3pz_3 was investigated as a potential scrubber for removal of DBT and DMDBT from isooctane. Firstly, addition of 1.3 equivalent of Ag_3pz_3 to a 10.0 mL of isooctane solution containing 100 mg/L S DBT or DMDBT resulted in the formation of a white precipitate, which was proved to be **Ag_3pz_3·DBT** or **Ag_3pz_3·DMDBT** based on ^{1}HNMR and PXRD measurements. Then, the remaining Ag_3pz_3 and DBT or DMDBT were extracted by 3×3.3 mL of acetonitrile. At last, the sample of Ag_3pz_3 can be recovered from **Ag_3pz_3·DBT** or **Ag_3pz_3·DMDBT** by column chromatography using silica gel as stationary phase; DBT or DMDBT can be firstly eluted out by using petroleum ether as eluent, while Ag_3pz_3 remains on the column, the latter of which can be obtained by eluting the column with ethyl acetate. As shown in Fig. S25 and Fig. S26, Ag_3pz_3 can be reused at least five times without obvious loss of desulfurizing efficiency, proving that Ag_3pz_3 is promising for practical applications. The ^{1}HNMR of the recovered sample of Ag_3pz_3 after five recycles is identical to that of as-synthesized sample.

X-ray Crystallography

Crystallographic data were collected on a Bruker AXS GmbH diffractometer with graphite monochromated Mo-Kα radiation (λ = 0.7107 Å) at 298 K for **Ag_3pz_3·BT** and **Ag_3pz_3·DMT**, and at 100 K for **Ag_3pz_3·DMDBT**; Crystallographic data was collected on an Agilent Technologies SuperNova Single Crystal Diffractometer equipped with graphite-monochromatic Mo-Kα radiation (λ = 0.71073 Å) at 120 K for **Ag_3pz_3·DBT**. Absorption corrections were obtained by using the multiscan program. All the structures were solved by direct methods with SHELXS and refined with the full-matrix least-squares technique using the SHELXL program[1] implemented through Olex2.[2] All non-hydrogen atoms were refined anisotropically, while the hydrogen atoms were generated geometrically. The crystallographic data are summarized in Table S12. CCDC: 1938383-1938386 for **Ag_3pz_3·DBT**, **Ag_3pz_3·DMDBT** **Ag_3pz_3·BT** and **Ag_3pz_3·DMT**, contains the supplementary crystallographic data for this paper, which can be obtained free of charge from the Cambridge Crystallographic Data Center.

Computational Details

The density functional theory (DFT) calculation, which has been widely applied in many kinds of computational studies, [3] was carried out with the Gaussian16 program.[4] The geometries were fully optimized using M06-L method[5] based on the X-ray diffraction data. In the calculation, basis set 6-31G(d, p) was used for H, C, N，F, and S atoms, while LANL2DZ was applied for Ag atom. [6]

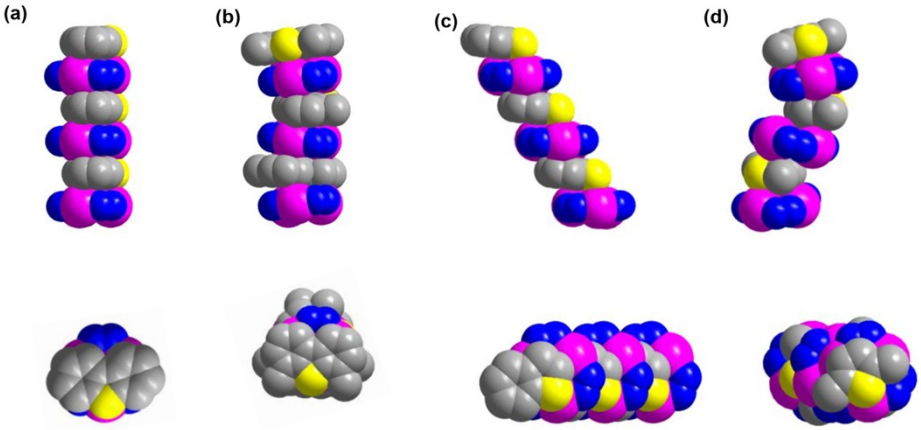

Fig. S1 The side view and top view of columnar stack of (a) **Ag_3pz_3·DBT**; (b) **Ag_3pz_3·DMDBT**; (c) **Ag_3pz_3·BT**; (d) **Ag_3pz_3·DMT**. Trifluoromethyl groups and hydrogen atoms have been omitted for clarity.

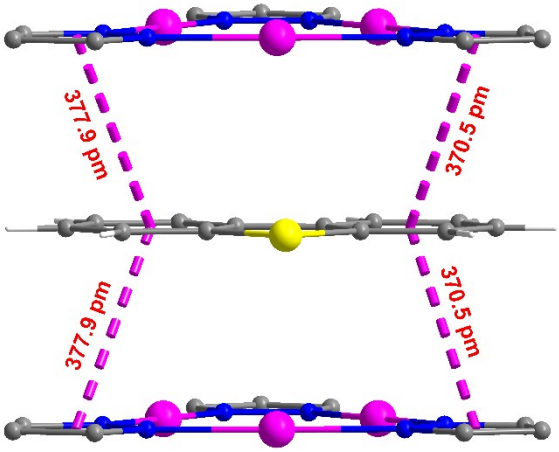

Fig. S2 The side view of **Ag_3pz_3·DBT** showing pyrazolyl-phenyl π-π interactions. Colour code: Ag, pink; N, blue; C, gray; H, white; S, yellow. The trifluoromethyl groups and hydrogen atoms of pyrazole have been omitted for clarity.

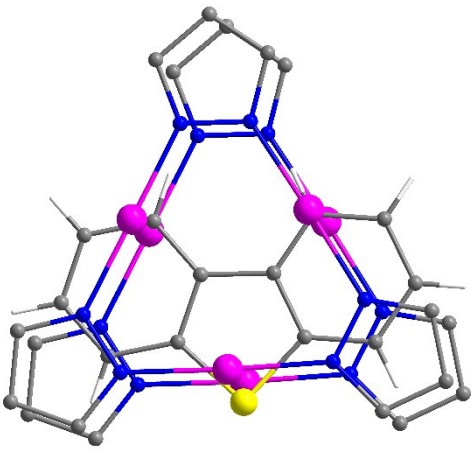

Fig. S3 The top view of **Ag_3pz_3·DBT**. Colour code: Ag, pink; N, blue; C, gray; H, white; S, yellow. The trifluoromethyl groups and hydrogen atoms of pyrazole have been omitted for clarity.

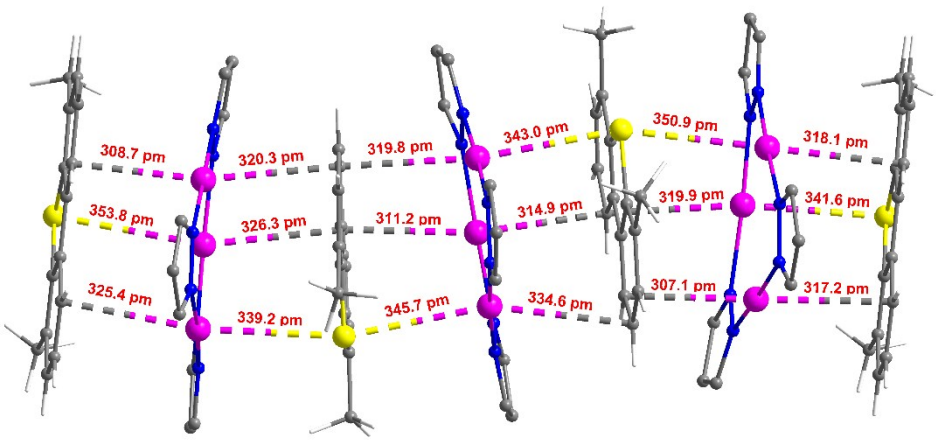

Fig. S4 The Ag···S and Ag···C contacts observed in the adduct of **Ag_3pz_3·DMDBT.** Colour code: Ag, pink; N, blue; C, gray; H, white; S, yellow. The trifluoromethyl groups and hydrogen atoms of pyrazole have been omitted for clarity.

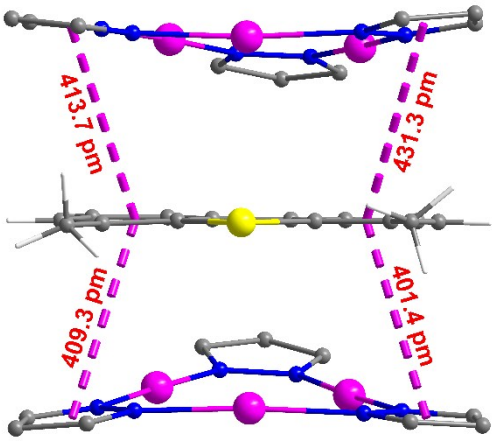

Fig. S5 The side view of **Ag_3pz_3·DMDBT** showing pyrazolyl-phenyl π-π interactions. Colour code: Ag, pink; N, blue; C, gray; H, white; S, yellow. The trifluoromethyl groups and hydrogen atoms of pyrazole have been omitted for clarity.

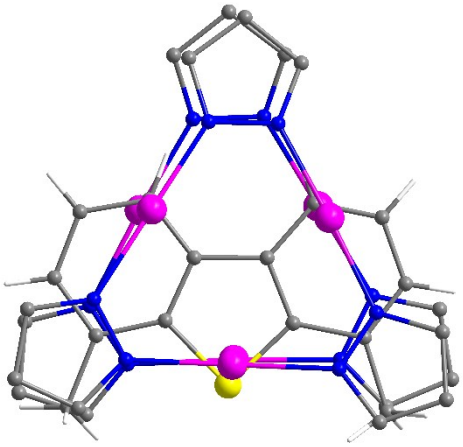

Fig. S6 The top view of **Ag_3pz_3·DMDBT**. Colour code: Ag, pink; N, blue; C, gray; H, white; S, yellow. The trifluoromethyl groups and hydrogen atoms of pyrazole have been omitted for clarity.

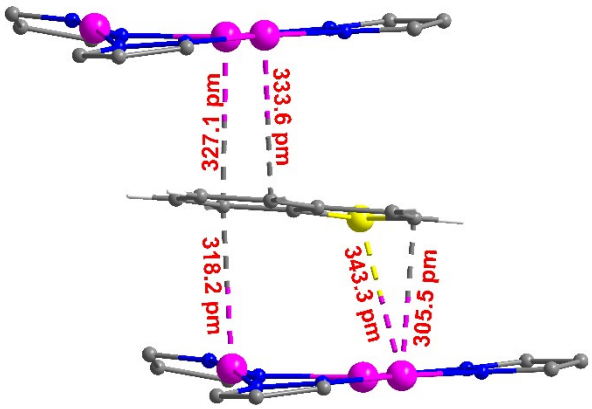

Fig. S7 A fragment of the displaced columnar stacking of **Ag_3pz_3·BT**, showing Ag···S and Ag···C contacts. Colour code: Ag, pink; N, blue; C, gray; H, white; S, yellow. The trifluoromethyl groups and hydrogen atoms of pyrazole have been omitted for clarity.

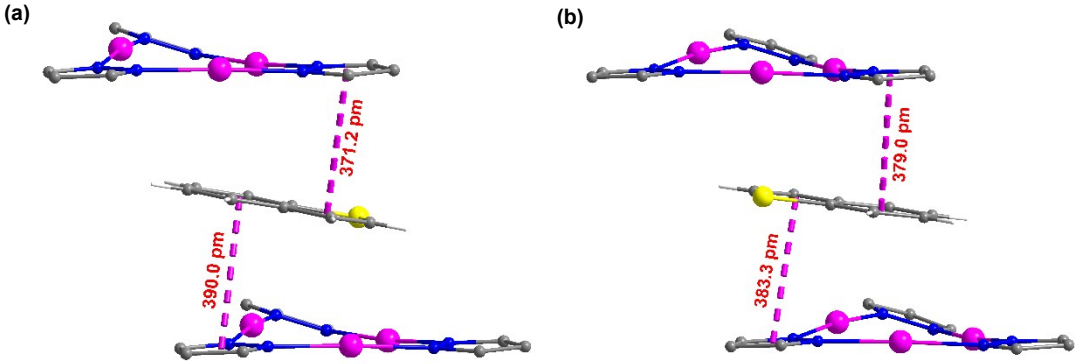

Fig. S8 The side view of **Ag_3pz_3·BT** showing pyrazolyl-phenyl and/or pyrazolyl-thiophene π-π interactions. Colour code: Ag, pink; N, blue; C, gray; H, white; S, yellow. The trifluoromethyl groups and hydrogen atoms of pyrazole have been omitted for clarity.

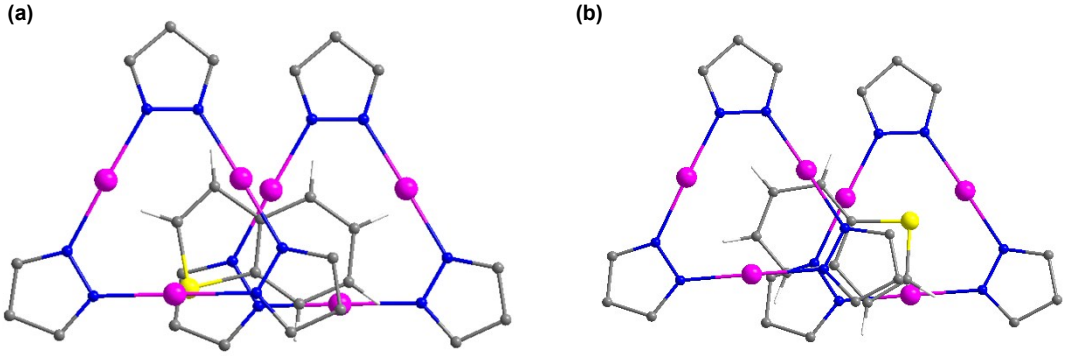

Fig. S9 The top view of **Ag_3pz_3·BT**. Colour code: Ag, pink; N, blue; C, gray; H, white; S, yellow. The trifluoromethyl groups and hydrogen atoms of pyrazole have been omitted for clarity.

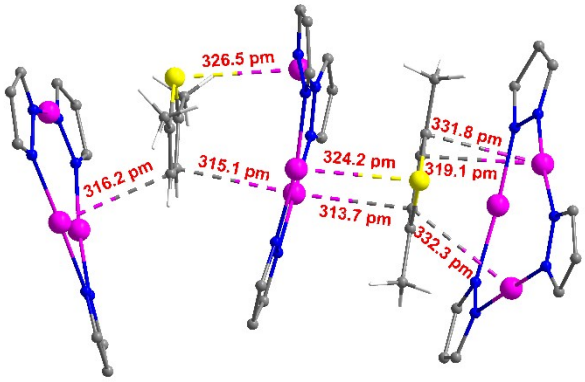

Fig. S10 The Ag···S and Ag···Ccontacts observed in the adduct of **Ag_3pz_3·DMT.** Colour code: Ag, pink; N, blue; C, gray; H, white; S, yellow. The trifluoromethyl groups and hydrogen atoms of pyrazole have been omitted for clarity.

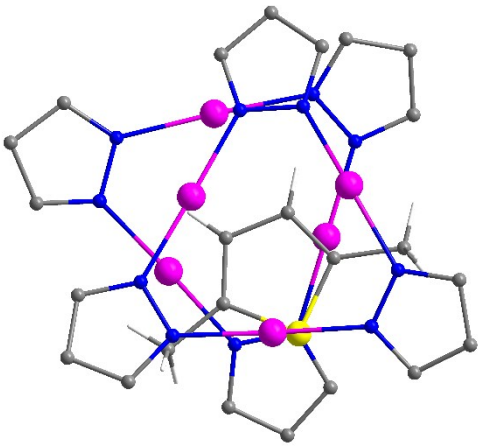

Fig. S11 The top view of **Ag_3pz_3·DMT.** Colour code: Ag, pink; N, blue; C, gray; H, white; S, yellow. The trifluoromethyl groups and hydrogen atoms of pyrazole have been omitted for clarity.

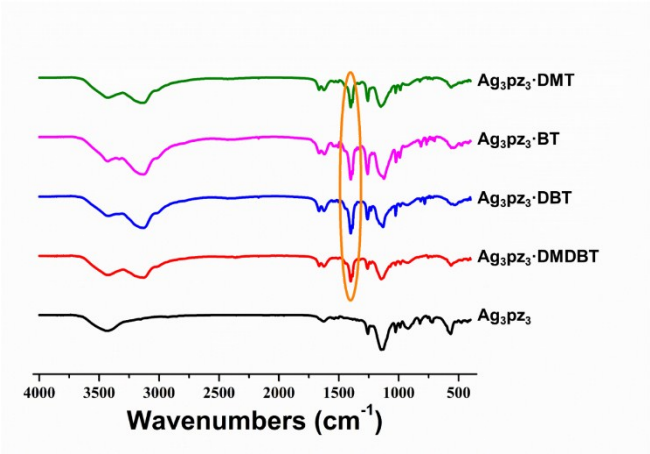

Fig. S12 IR spectra (KBr pellet) of **Ag_3pz_3** and adducts. The peak of near 1400 cm^{-1} corresponds to the stretching vibration of the thiophenyl ring in the adducts. [7-9]

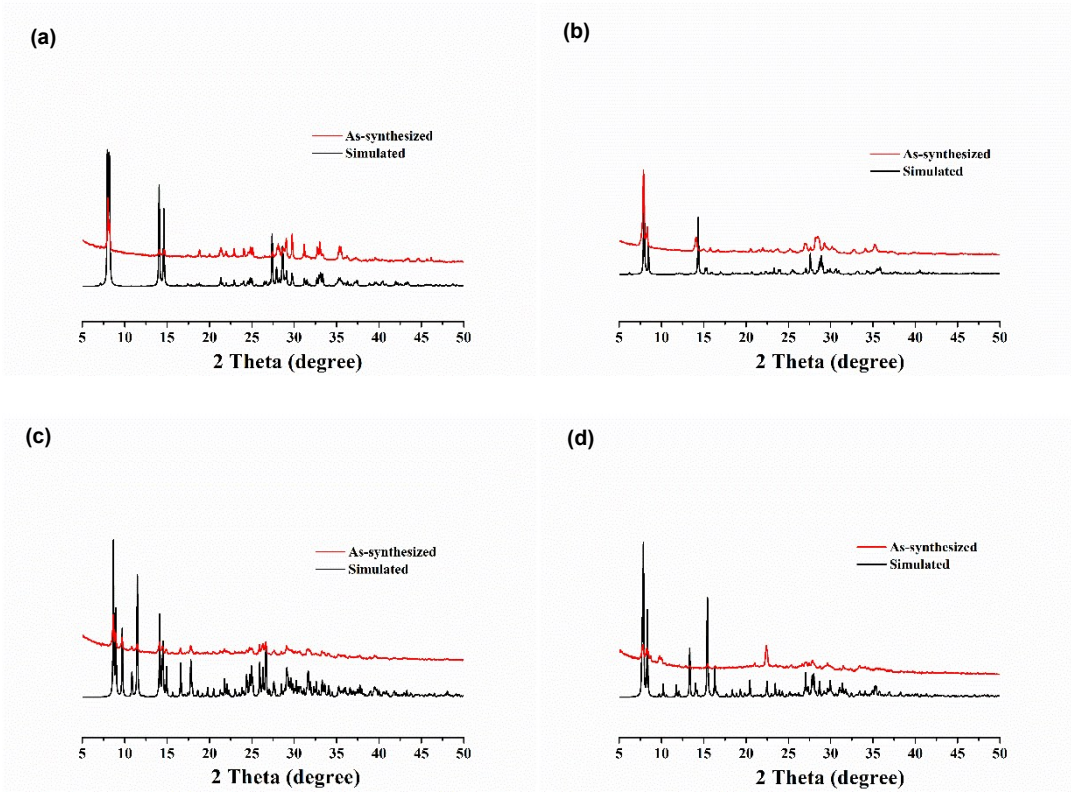

Fig. S13 The P-XRD patterns of (a) **Ag_3pz_3·DBT**; (b) **Ag_3pz_3·DMDBT**; (c) **Ag_3pz_3·BT**; (d) **Ag_3pz_3·DMT**, obtained from the as-synthesized sample (red line) or simulated based on the crystal data (black line).

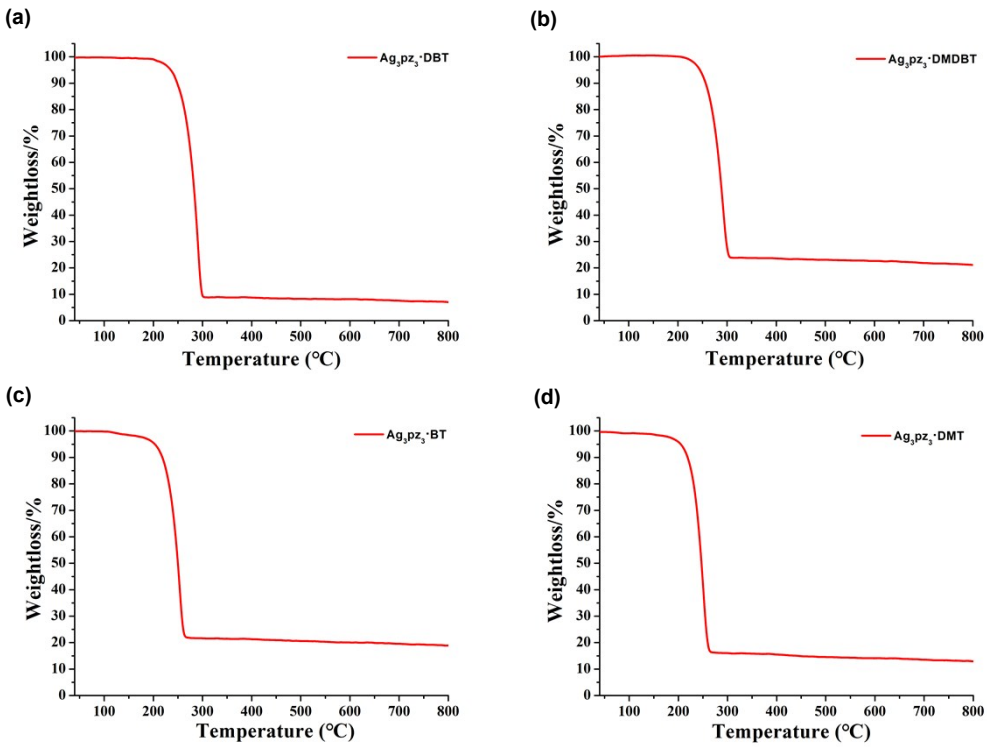

Fig. S14 Thermogravimetric curves of (a) **Ag_3pz_3·DBT**; (b) **Ag_3pz_3·DMDBT**; (c) **Ag_3pz_3·BT**; (d) **Ag_3pz_3·DMT**.

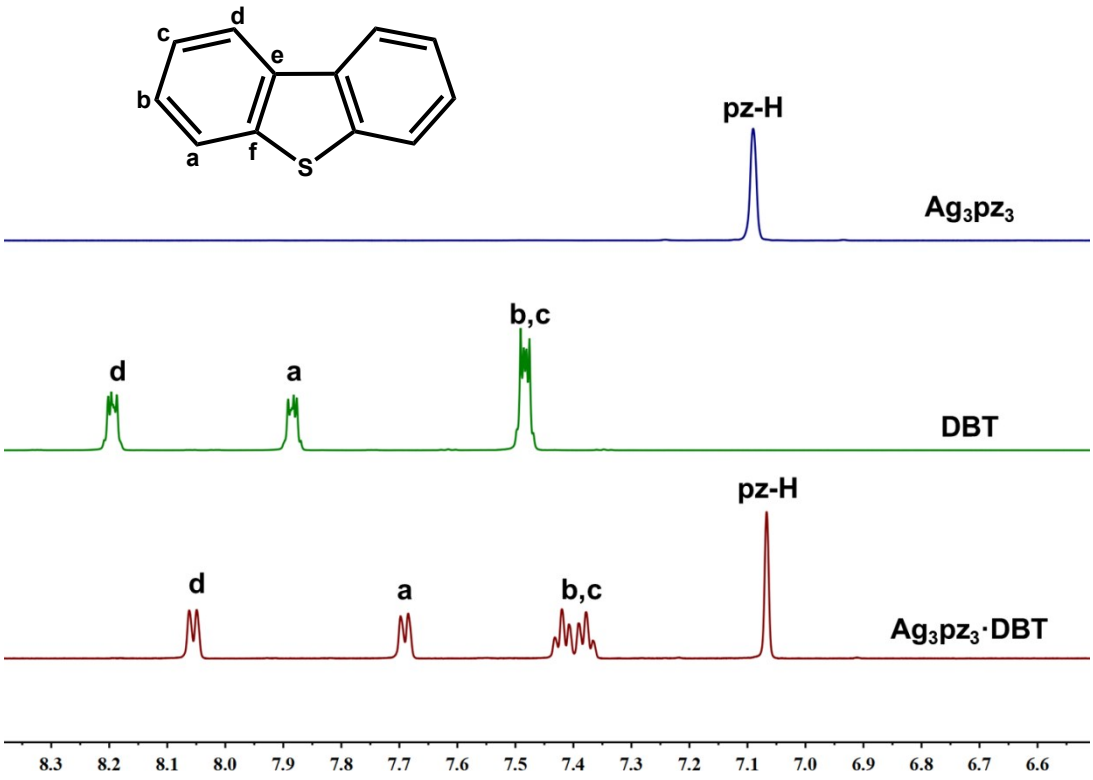

Fig. S15 Stack plot of ^{1}H NMR spectra for **Ag_3pz_3**, DBT and **Ag_3pz_3·DBT** in CD_2Cl_2.

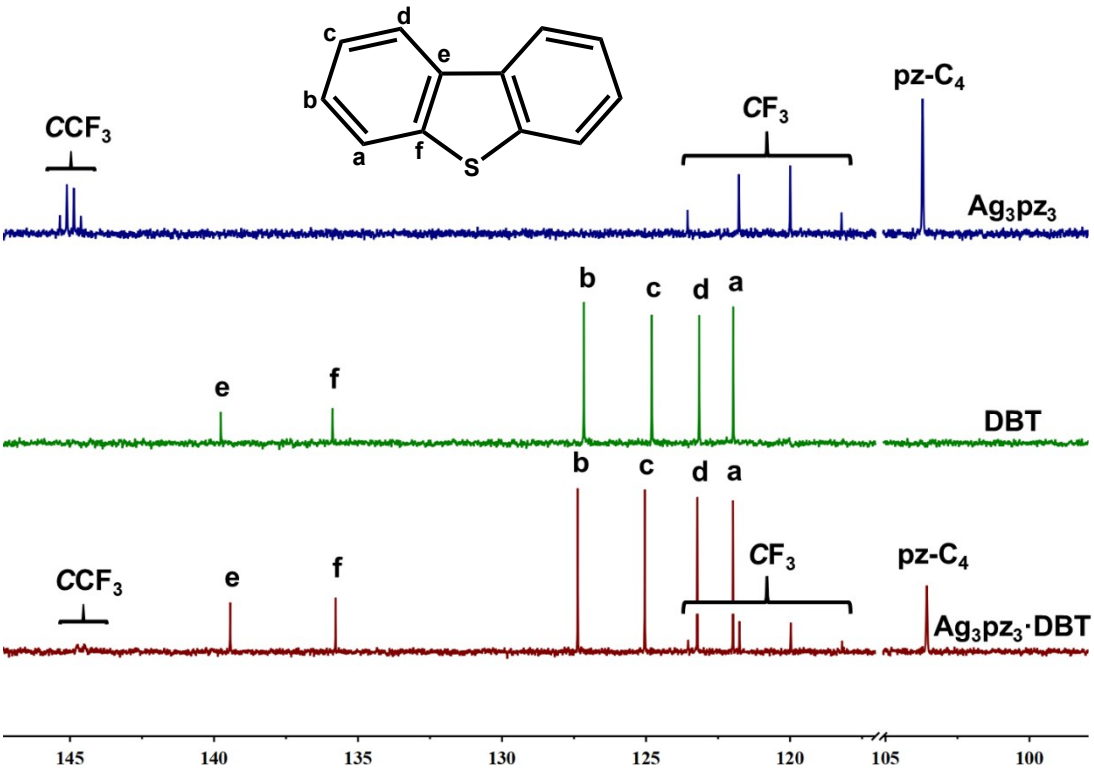

Fig. S16 Stack plot of ^{13}C NMR spectra for **Ag_3pz_3**, DBT and **Ag_3pz_3·DBT** in CD_2Cl_2.

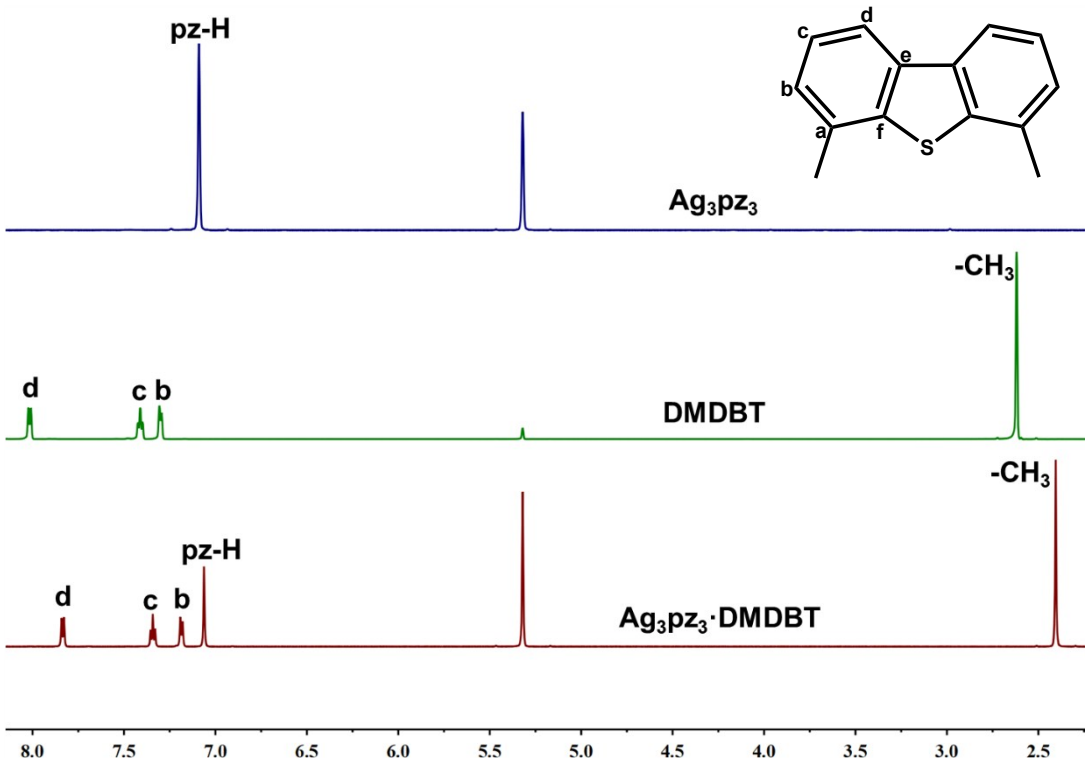

Fig. S17 Stack plot of ^{1}H NMR spectra for **Ag_3pz_3**, DMDBT and **Ag_3pz_3·DMDBT** in CD_2Cl_2.

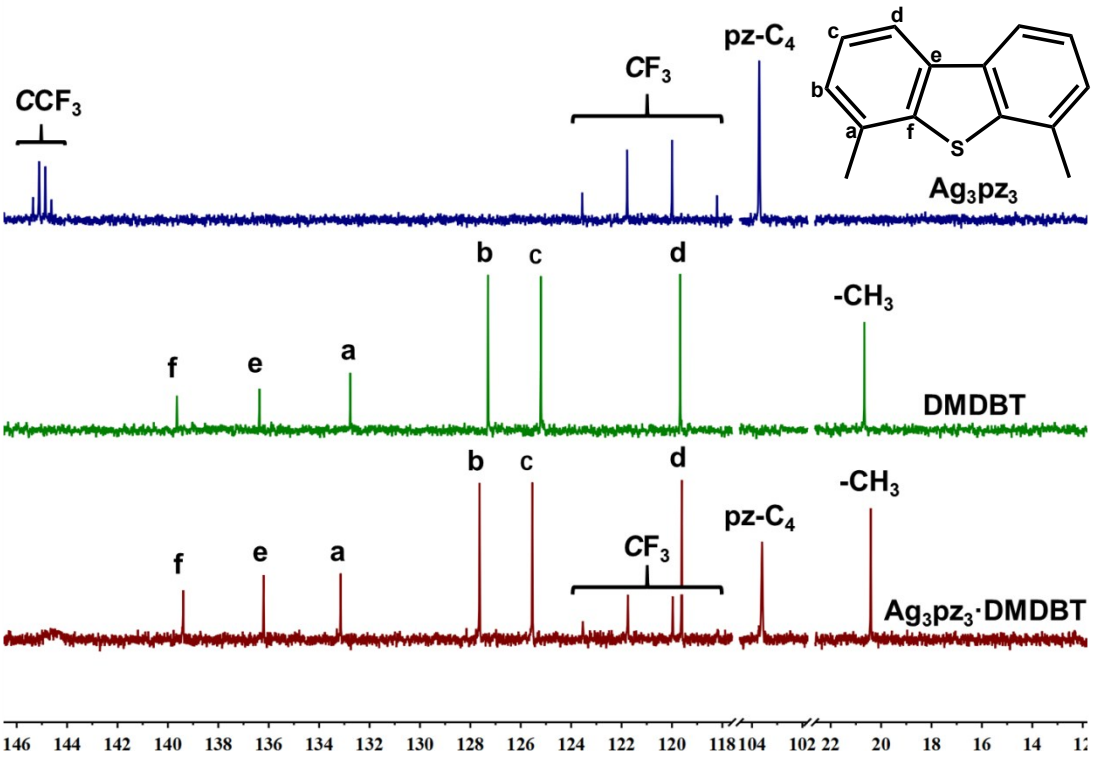

Fig. S18 Stack plot of ^{13}C NMR spectra for **Ag_3pz_3**, DMDBT and **Ag_3pz_3·DMDBT** in CD_2Cl_2.

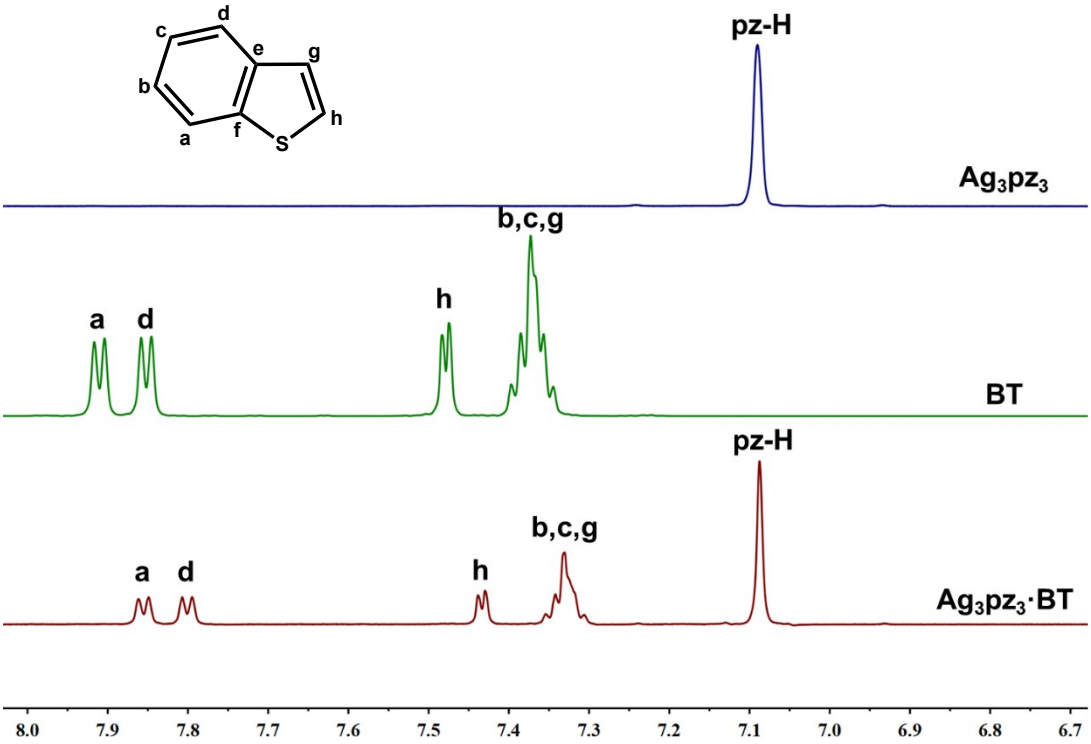

Fig. S19 Stack plot of ^{1}H NMR spectra for **Ag_3pz_3**, BT and **Ag_3pz_3·BT** in CD_2Cl_2.

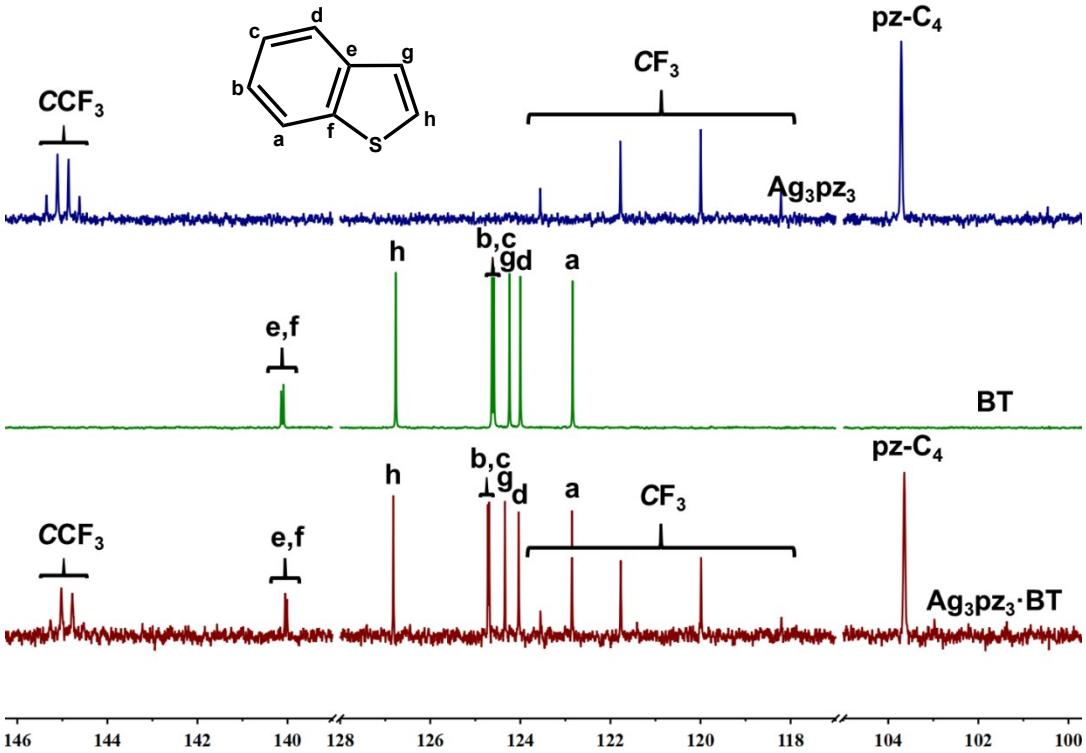

Fig. S20 Stack plot of ^{13}C NMR spectra for **Ag_3pz_3**, BT and **Ag_3pz_3·BT** in CD_2Cl_2.

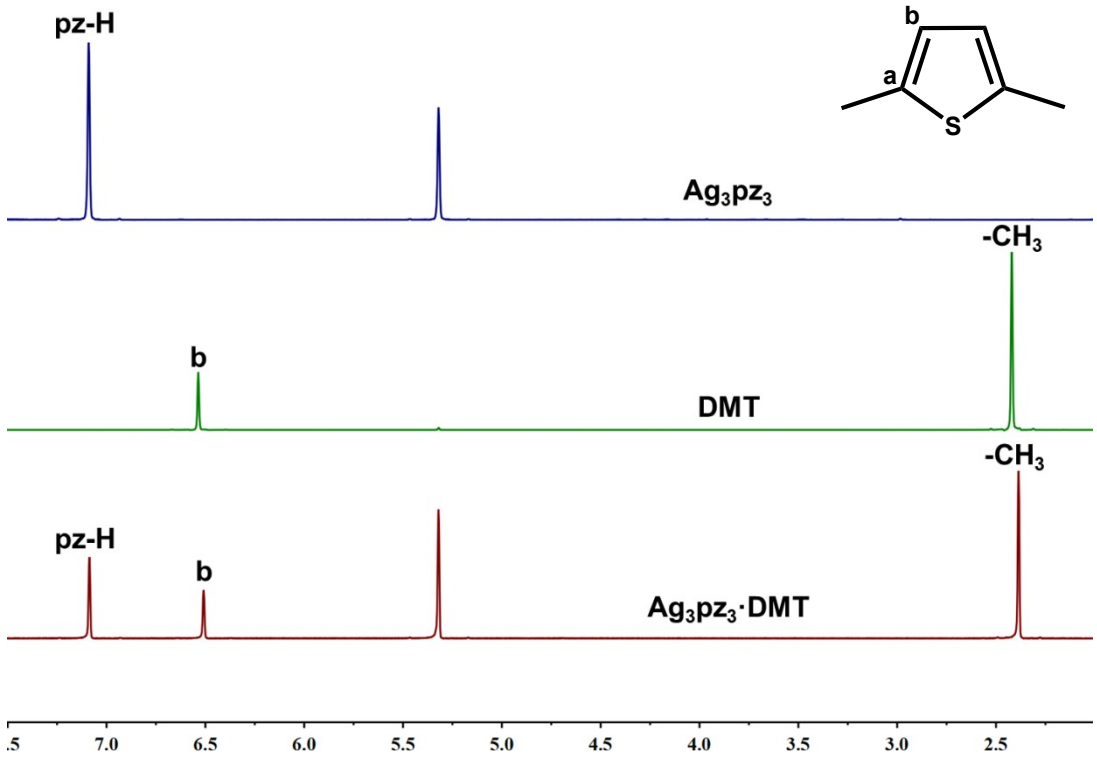

Fig. S21 Stack plot of ^{1}H NMR spectra for **Ag_3pz_3**, DMT and **Ag_3pz_3·DMT** in CD_2Cl_2.

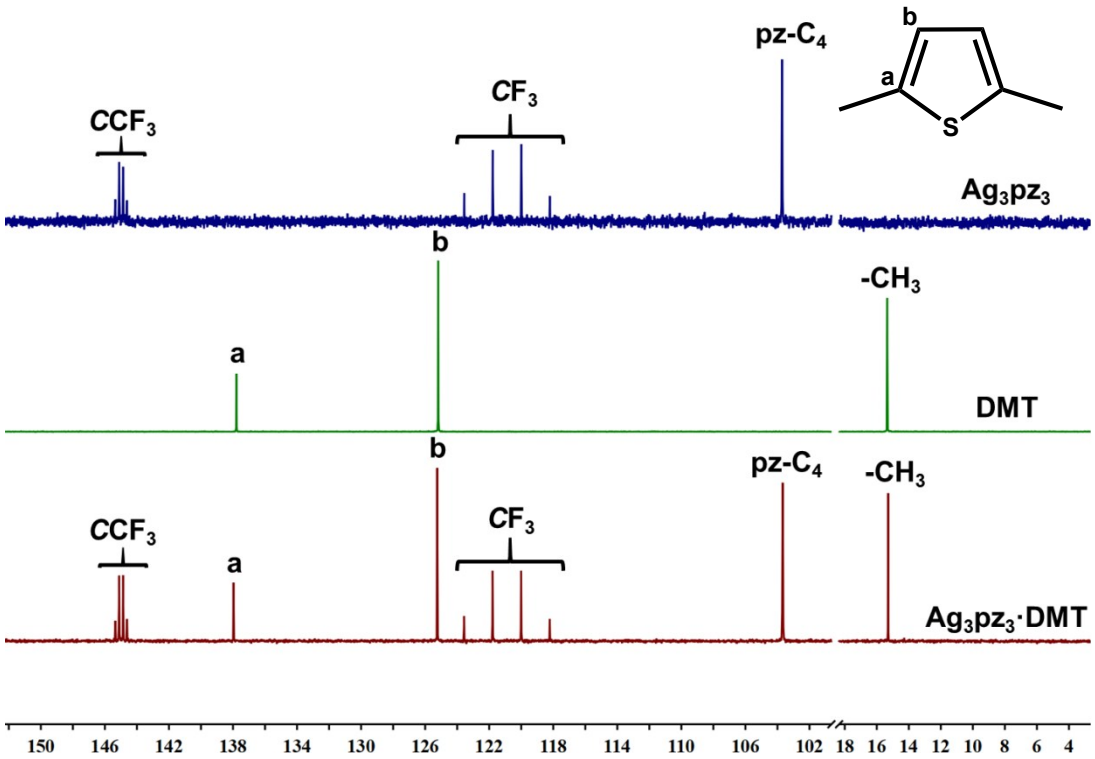

Fig. S22 Stack plot of ^{13}C NMR spectra for **Ag_3pz_3**, DMT and **Ag_3pz_3·DMT** in CD_2Cl_2.

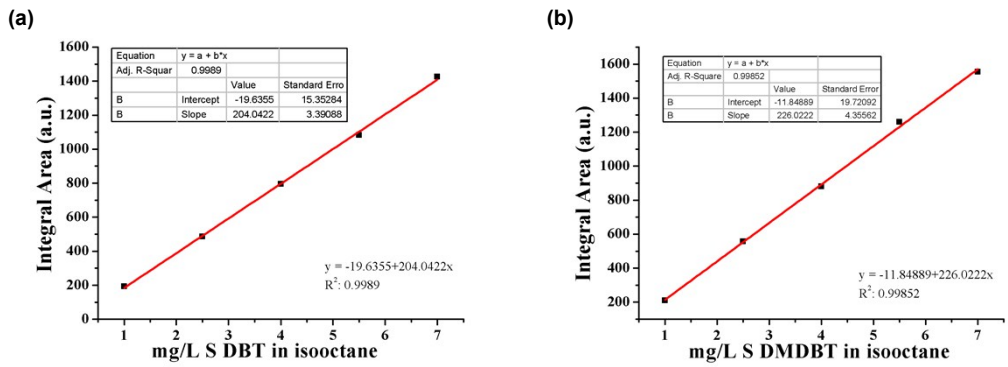

Fig. S23 Standard curve of DBT (a) and DMDBT (b) in isooctane in the range of 1.0-7.0 mg/L S based on HPLC.

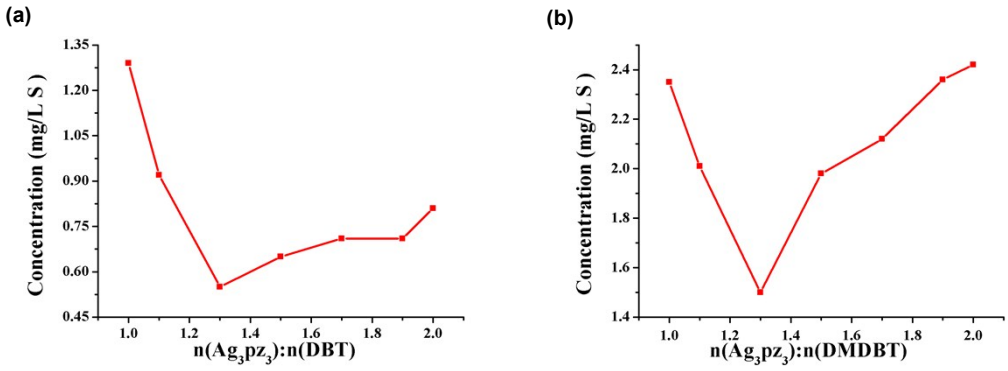

Fig. S24 The remaining sulfur concentrations measured after the addition of $\mathbf{Ag_3pz_3}$ into the model oil containing DBT(a) or DMDBT(b), indicating desulfurization performance is optimal when the molar ratio of $\mathbf{Ag_3pz_3}$: DBT (or DMDBT) = 1.3 : 1.

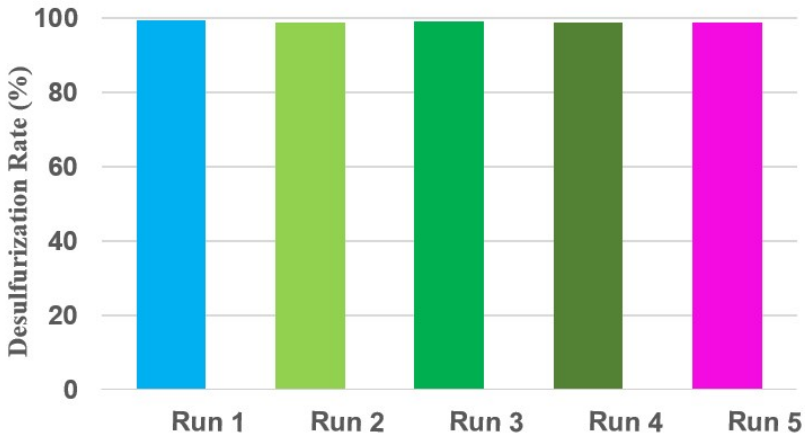

Fig. S25 Recycling test of $\mathbf{Ag_3pz_3}$ for the removal of DBT from isooctane.

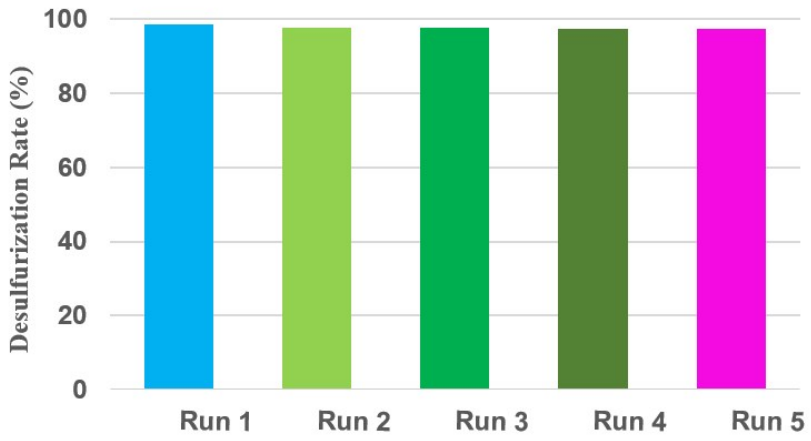

Fig. S26 Recycling test of **Ag_3pz_3** for the removal of DMDBT from isooctane.

Table S1. A summary of Ag···S, Ag···C contacts and the π-π interactions in the adducts.

	Ag_3pz_3·DBT	**Ag_3pz_3·DMDBT**	**Ag_3pz_3·BT**	**Ag_3pz_3·DMT**
Ag···S (Å)	3.2032(11); 3.2224(13); 3.2118(12)	3.3921(23); 3.4163(21); 3.4296(19); 3.4566(20); 3.5091(22); 3.5376(24);	3.228(11); 3.433(11)	3.2421(30); 3.2646(33)
Average (Å)	3.2125	3.4569 The steric hindrance of the two methyl groups is too large, causing the distance to be longer than other Ag···S distances	3.331	3.2534
Ag···C (Å)	3.1668(25); 3.1669(25); 3.1690(26); 3.1774(21); 3.1909(28); 3.2064(37)	3.0708(90); 3.0872(96); 3.1118(84); 3.1492(73); 3.1725(93); 3.1807(97); 3.1981(90); 3.1993(78); 3.2032(83); 3.254(10); 3.2629(77); 3.346(11)	3.055(23); 3.182(16); 3.203(17); 3.271(16); 3.284(16); 3.305(13); 3.336(16); 3.351(17);	3.1624(76); 3.1514(86); 3.1374(84); 3.3181(57); 3.1914(77); 3.3234(93);
Average (Å)	3.1796	3.1863	3.248	3.2140
Phenyl (thienyl)-pyrazolyl π-π stacking (Å)	3.6763(1); 3.8143(1); 3.7788(1); 3.7047(1); 3.9036(1); 3.6818(1)	3.8926(2); 3.9511(2); 3.9848(2); 4.0087(2); 4.0139(2); 4.0606(2); 4.0839(2); 4.0929(2); 4.1368(2); 4.2338(2); 4.3127(2); 4.3535(2);	3.7122; 3.7902; 3.8328; 3.9004	
Average (Å)	3.7599	4.0938 The steric hindrance of the two methyl groups is too large, causing the distance to be longer than other distances of phenyl-pyrazolyl π-π stacking	3.8089	

Table S2. Comparison of ^{1}H NMR of **Ag_3pz_3**, DBT and **Ag_3pz_3·DBT.**

^{1}H NMR /ppm	pz-H	d	a	b,c
DBT		8.20(m)	7.89(m)	7.49(m)
Ag_3pz_3	7.09(s)			
Ag_3pz_3·DBT	7.07(s)	8.06(d)	7.69(t)	7.40(dt)
Δ/ppm	0.02	0.14	0.13	0.09

Table S3. Comparison of ^{13}C NMR of **Ag_3pz_3**, DBT and **Ag_3pz_3·DBT**.

^{13}C NMR /ppm	*C*CF_3	*C*F_3	pz-C_4	e	f	b	c	d	a
DBT				139.76	135.89	127.16	124.80	123.16	121.97
Ag_3pz_3	144.99	120.89	103.71						
Ag_3pz_3·DBT		120.86	103.57	139.44	135.78	127.37	125.04	123.22	121.98
Δ/ppm		0.03	0.14	0.32	0.11	-0.21	-0.24	-0.06	-0.01

Table S4. Comparison of ^{1}H NMR of **Ag_3pz_3**, DMDBT and **Ag_3pz_3·DMDBT**.

^{1}H NMR /ppm	pz-H	d	c	b	-CH_3
DMDBT		8.02(d)	7.41(t)	7.30(d)	2.62(s)
Ag_3pz_3	7.09(s)				
Ag_3pz_3·DMDBT	7.07(s)	7.84(d)	7.34(t)	7.19(d)	2.41(s)
Δ/ppm	0.02	0.18	0.07	0.11	0.21

Table S5. Comparison of ^{13}C NMR of **Ag_3pz_3**, DMDBT and **Ag_3pz_3·DMDBT**.

^{13}C NMR /ppm	*C*CF_3	*C*F_3	pz-C_4	f	e	a	b	c	d	-CH_3
DMDBT				139.64	136.37	132.77	127.30	125.20	119.67	20.66
Ag_3pz_3	144.99	120.89	103.71							
Ag_3pz_3·DMDBT		120.86	103.60	139.39	136.20	133.15	127.64	125.54	119.56	20.41
Δ/ppm		0.03	0.11	0.25	0.17	-0.38	-0.34	-0.34	0.11	0.25

Table S6. Comparison of ^{1}H NMR of**Ag_3pz_3**, BT and **Ag_3pz_3·BT**.

^{1}H NMR /ppm	pz-H	a	d	h	b,c,g
BT		7.91(d)	7.86(d)	7.48(d)	7.37(m)
Ag_3pz_3	7.09(s)				
Ag_3pz_3·BT	7.09(s)	7.86(d)	7.80(d)	7.43(d)	7.33(m)
Δ/ppm	0	0.05	0.06	0.05	0.04

Table S7. Comparison of ^{13}C NMR of **Ag_3pz_3**, BT and **Ag_3pz_3·BT**.

^{13}C NMR /ppm	*C*CF_3	*C*F_3	pz-C_4	f	e	h	b	c	g	d	a
BT				140.14	140.09	126.77	124.63	124.59	124.24	124.00	122.84
Ag_3pz_3	144.99	120.89	103.71								
Ag_3pz_3·BT	144.90	120.87	103.65	140.05	140.01	126.82	124.72	124.69	124.34	124.04	122.85
Δ/ppm	0.09	0.02	0.06	0.09	0.08	-0.05	-0.09	-0.10	-0.10	-0.04	-0.01

Table S8. Comparison of ^{1}H NMR of **Ag_3pz_3**, DMT and **Ag_3pz_3·DMT**.

^{1}H NMR /ppm	pz-H	b	-CH_3
DMT		6.54(s)	2.42(s)
Ag_3pz_3	7.09(s)		
Ag_3pz_3·DMT	7.09(s)	6.51(s)	2.39(s)
Δ/ppm	0	0.03	0.03

Table S9. Comparison of ^{13}C NMR of **Ag_3pz_3**, DMT and **Ag_3pz_3·DMT**.

^{13}C NMR /ppm	*C*CF_3	*C*F_3	pz-C_4	a	b	-CH_3
DMT				137.79	125.18	15.35
Ag_3pz_3	144.99	120.89	103.71			
Ag_3pz_3·DMT	144.99	120.90	103.67	137.96	125.24	15.29
Δ/ppm	0	-0.01	0.04	-0.17	-0.06	0.06

Table S10. The Gibbs free energy of **Ag_3pz_3**, HASC molecules and their adducts obtained by DFT-calculation.

	Gibbs free energy (a.u.)	Binding energy (ΔG) (Kcal/mol)
Ag_3pz_3	-3136.282714	
DBT	-860.118069	
Ag_3pz_3·DBT	-3996.422098	-13.38
DMDBT	-938.700159	
Ag_3pz_3·DMDBT	-4075.003656	-13.05
BT	-706.522071	
Ag_3pz_3·BT	-3842.81873	-8.76
DMT	-631.507767	
Ag_3pz_3·DMT	-3767.801914	-7.18

Table S11. Selected bond distances (Å) and bond angles (º).

Ag_3pz_3·DBT			
Ag(1)-N(1)	2.074(11)	Ag(1)-N(6)	2.071(11)
Ag(2)-N(2)	2.070(11)	Ag(2)-N(3)	2.099(12)
Ag(3)-N(4)	2.090(12)	Ag(3)-N(5)	2.096(12)
Ag(1)···Ag(2)	3.4994(13)	Ag(2)···Ag(3)	3.4821(14)
Ag(3)···Ag(2)	3.4685(14)	S(1A)···Ag(1)	3.2224(13)
S(2)···Ag(2)	3.2118(12)	S(3)···Ag(3)	3.2032(11)
C(23C)···Ag(2)	3.1690(26)	C(20C)···Ag(1)	3.2064(37)
C(23B)···Ag(1)	3.1668(25)	C(20B)···Ag(3)	3.1774(21)
C(23A)···Ag(3)	3.1909(28)	C(20A)···Ag(2)	3.1669(25)
N(1)-Ag(1)-N(6)	178.5(4)	N(2)-Ag(2)-N(3)	177.5(4)
N(4)-Ag(3)-N(5)	179.8(5)		
Ag_3pz_3·DMDBT			
Ag(1)-N(1)	2.119(6)	Ag(1)-N(6)	2.075(6)
Ag(2)-N(2)	2.081(7)	Ag(2)-N(3)	2.112 (6)
Ag(3)-N(4)	2.108(7)	Ag(3)-N(5)	2.079(8)
Ag(4)-N(7)	2.137(7)	Ag(4)-N(12)	2.085(7)
Ag(5)-N(8)	2.102(7)	Ag(5)-N(9)	2.098(6)
Ag(6)-N(10)	2.059(8)	Ag(6)-N(11)	2.079(7)
Ag(7)-N(13)	2.125(6)	Ag(7)-N(18)	2.085(6)
Ag(8)-N(14)	2.100(7)	Ag(8)-N(15)	2.109(7)
Ag(9)-N(16)	2.103(7)	Ag(9)-N(17)	2.128(6)
Ag(1)···Ag(2)	3.4960(9)	Ag(2)···Ag(3)	3.5442(10)
Ag(3)···Ag(1)	3.4011(8)	Ag(4)···Ag(5)	3.4861(9)
Ag(5)···Ag(6)	3.4481(10)	Ag(6)···Ag(4)	3.5151(9)
Ag(7)···Ag(8)	3.4434(10)	Ag(8)···Ag(9)	3.4766(10)
Ag(9)···Ag(7)	3.5011(9)	S(1)···Ag(1)	3.4163(21)
S(1)···Ag(7)$^{\#}$	3.5376(24)	S(2)···Ag(3)	3.5091(22)
S(2)···Ag(6)	3.4296(19)	S(3)···Ag(5)	3.4566(20)
S(3)···Ag(8)	3.3921(23)	C(69)···Ag(1)	3.1993(78)
C(55)···Ag(2)	3.1725(93)	C(67)···Ag(2)	3.0708(90)
C(53)···Ag(3)	3.1807(97)	C(69)···Ag(4)	3.1492(73)
C(83)···Ag(4)	3.1118(84)	C(66)···Ag(5)	3.346(11)
C(81)···Ag(6)	3.1981(90)	C(83)···Ag(7)	3.2629(77)
C(55)$^{\#}$···Ag(8)	3.254(10)	C(81)···Ag(9)	3.2032(83)
C(53)$^{\#}$···Ag(9)	3.0872(96)	N(1)-Ag(1)-N(6)	176.9(2)
N(2)-Ag(2)-N(3)	176.4(3)	N(4)-Ag(3)-N(5)	178.1(2)
N(7)-Ag(4)-N(12)	177.2(34)	N(8)-Ag(5)-N(9)	176.0(3)
N(10)-Ag(6)-N(11)	176.2(2)	N(13)-Ag(7)-N(18)	178.1(2)
N(14)-Ag(8)-N(15)	175.6(3)	N(16)-Ag(9)-N(17)	177.6(2)
#: 1+x, -1+y, -1+z			
Ag_3pz_3·BT			
Ag(1)-N(1)	2.101(7)	Ag(1)-N(6)	2.099(6)

Ag(2)-N(2)	2.100(7)	Ag(2)-N(3)	2.100(7)
Ag(3)-N(4)	2.096 (6)	Ag(3)-N(5)	2.089(6)
Ag(1)…Ag(2)	3.4266(10)	Ag(2)···Ag(3)	3.4693(10)
Ag(3)···Ag(1)	3.4234(11)	S(1A)···Ag(1)#	3.228(11)
S(1B)···Ag(1)	3.433(11)	C(22A)···Ag(2)#	3.351(18)
C(18A)···Ag(1)	3.203(17)	C(21A)···Ag(3)	3.305(13)
C(20A)···Ag(3)	3.282(16)	C(23B)···Ag(1)	3.055(23)
C(17B)···Ag(3)	3.182(16)	C(20B)···Ag(1)	3.336(16)
C(17B)···Ag(2)	3.271(16)	N(1)-Ag(1)-N(6)	178.0(3)
N(2)-Ag(2)-N(3)	174.9(3)	N(4)-Ag(3)-N(5)	174.2(3)
#: -1+x, y, z			
Ag_3pz_3·DMT			
Ag(1)-N(1)	2.085(6)	Ag(1)-N(6)	2.099(8)
Ag(2)-N(2)	2.084(6)	Ag(2)-N(3)	2.084(6)
Ag(3)-N(4)	2.084(6)	Ag(3)-N(5)	2.101(8)
Ag(4)-N(7)	2.095(6)	Ag(4)-N(12)	2.093(6)
Ag(5)-N(8)	2.088(5)	Ag(5)-N(9)	2.081(6)
Ag(6)-N(10)	2.099(6)	Ag(6)-N(11)	2.098(5)
Ag(1)···Ag(2)	3.3697(7)	Ag(2)···Ag(3)	3.4020(8)
Ag(3)···Ag(1)	3.4567(11)	Ag(4)···Ag(5)	3.3651(7)
Ag(5)···Ag(6)	3.4838(9)	Ag(6)···Ag(4)	3.4352(6)
S(1)···Ag(3)	3.2646(33)	S(2)···Ag(1)#	3.2421(30)
C(34)···Ag(2)	3.1514(86)	C(39) ···Ag(2)#	3.1374(84)
C(33)···Ag(4)	3.1624(76)	C(39)···Ag(4)	3.3234(93)
C(40)···Ag(5)	3.1914(77)	C(41)···Ag(5)	3.3181(57)
N(1)-Ag(1)-N(6)	171.4(3)	N(2)-Ag(2)-N(3)	178.6(2)
N(4)-Ag(3)-N(5)	169.8(3)	N(7)-Ag(4)-N(12)	177.7(2)
N(8)-Ag(5)-N(9)	174.6(2)	N(10)-Ag(6)-N(11)	174.8(2)
#: x, 1.5-y, -0.5+z			

Table S12. Crystallographic data and structure refinements.

	Ag_3pz_3·DBT	**Ag_3pz_3·DMDBT**	**Ag_3pz_3·BT**	**Ag_3pz_3·DMT**
Formula	$C_{27}H_{11}Ag_3F_{18}N_6S$	$C_{29}H_{15}Ag_3F_{18}N_6S$	$C_{23}H_9Ag_3F_{18}N_6S$	$C_{21}H_{11}Ag_3F_{18}N_6S$
Mol. wt.	1117.09	1145.14	1067.03	1045.03
Crystal system	Monoclinic	Triclinic	Monoclinic	Monoclinic
Space group	*C*2/m	*P*1	$P2_1$/c	$P2_1$/c
a (Å)	24.4726(12)	13.1618(8)	7.7008(10)	21.9258(5)
b (Å)	6.3315(3)	15.6344(9)	10.1698(2)	13.2224(3)
c (Å)	22.0593(10)	15.6527(9)	40.8111(7)	23.7561(6)
α (deg)		83.7474(7)		
β (deg)	90.630(5)	65.3474(7)	92.2883(6)	105.2918(9)
γ (deg)		65.8734(6)		
V (Å^3)	3417.8(3)	2664.3(3)	3193.60(9)	6643.3(3)
Z	4	3	4	8
T (K)	120	100	298	298
$\rho_{calcd.}$ (Mg/m^3)	2.171	2.141	2.219	2.090
μ (mm^{-1})	1.893	1.824	2.020	1.939
Reflns collected	6284	21246	47098	112579
Reflns unique	3312 (R_{int} = 0.0309)	17932 (R_{int} = 0.0185)	7447 (R_{int} = 0.0502)	15297 (R_{int} = 0.0794)
Final *R* indices	R_1 =0.0743	R_1 = 0.0443	R_1 = 0.0643	R_1 = 0.0551
[$I > 2\sigma(I)$]	wR_2 = 0.1655	wR_2 = 0.1070	wR_2 = 0.1842	wR_2 = 0.1346
S	1.071	1.056	1.024	1.006
$\Delta\rho_{max}$(eÅ^{-3})	2.57	1.34	1.61	0.67
$\Delta\rho_{min}$(eÅ^{-3})	-2.25	-1.16	-1.35	-0.55

References

1. G. M. Sheldrick, *Acta Cryst.*, 2008, **A64**, 112.
2. O. V. Dolomanov, L. J. Bourhis, R. J. Gildea, J. A. K. Howard and H. Puschmann, *J. Appl. Cryst.*, 2009, **42**, 339.
3. a) D. Wei, B. Lei, M. Tang and C.-G. Zhan, *J. Am. Chem. Soc.*, 2012, *134*, 10436; b) X.-K. Guo, L.-B. Zhang, D. Wei and J.-L. Niu, *Chem. Sci.*, 2015, **6**, 7059.
4. M. J. Frisch, G. W. Trucks, H. B. Schlegel, G. E. Scuseria, M. A. Robb, J. R. Cheesman, J. A. Montgomery, T. Vreven, K. N. Kudin, J. C. Burant, J. M. Millam, S. S. Iyengar, J. Tomasi and V. Barone, et al., Gaussian16, Gaussian Inc., Wallingford, CT, 2017.
5. Y. Zhao and D. G. Truhlar, *J. Chem. Phys.*, 2006, **125**, 194101.
6. P. J. Hay and W. R. Wadt, *J. Chem. Phys.*, 1985, **82**, 299.
7. S. Hotta, S. D. D. V. Rughooputh, A. J. Heeger and F. Wudl, *Macromolecules*, 1987, **20**, 212.
8. Z. W. Sun and A. J. Frank, *J. Chem. Phys.*, 1991, **94**, 4600.
9. M. Lanzi, P. C. Bizzarri, L. Paganin and G. Cesari, *Synth. Met.*, 2007, **157**, 719.